

Origin of the High-Frequency Resonances in ^1H NMR Spectra of Muscle Tissue: An in Vitro Slow Magic-Angle Spinning Study

HANNE CHRISTINE BERTRAM,^{*,†} HANS JØRGEN JAKOBSEN,[§] AND
 OLE BÆKGAARD NIELSEN[#]

Department of Food Science, Danish Institute of Agricultural Sciences, Research Centre Foulum, P.O. Box 50, DK-8830 Tjele, Denmark; Instrument Centre for Solid-State NMR Spectroscopy, Department of Chemistry, University of Aarhus, Langelandsgade 140, DK-8000 Aarhus C, Denmark; and Institute of Physiology and Biophysics, University of Aarhus, DK-8000 Aarhus C, Denmark

High-resolution slow magic-angle spinning (150 Hz) ^1H PASS NMR spectroscopy is performed on intact excised rat m. tibialis anterior. Untreated muscles and muscles in vitro incubated in Krebs–Ringers buffer based on deuterium oxide are investigated. In the high-frequency region of the ^1H NMR spectra, resonances from H4 (~7.1–7.2 ppm) and H2 (~8.2–8.5 ppm) in histidine are observed. In addition, a resonance appears at 6.7 ppm for the untreated muscles. However, this resonance is absent in muscles following incubation in deuterium oxide. On the basis of its behavior in deuterium oxide combined with supplementary measurements for creatine solutions, the 6.7 ppm resonance is ascribed to the amino protons in creatine. Moreover, the present study demonstrates that the observation of the 6.7 ppm resonance depends on pH, which explains earlier reports stating its occasional appearance. Finally, measurements on solutions of ATP/AMP and histidine indicate that both ATP/AMP and histidine contribute to the resonances at ~8.2–8.5 ppm in the ^1H NMR spectra of muscle tissue.

KEYWORDS: Creatine; histidine; ATP; post-mortem muscle; pH; MAS; high-resolution ^1H NMR spectroscopy; PASS

INTRODUCTION

Recent advances in spectral resolution for ^1H NMR spectra of tissues employing magic-angle spinning (MAS) have resulted in promising results, suggesting that the technique may be a useful diagnostic tool (1–10). However, a prerequisite for optimal use of the information contained in these ^1H spectra is identification of the various resonances appearing in the spectra. In the low-frequency region of ^1H NMR spectra of muscle tissues, several lines appear that have been assigned to various protons in lipids, amino acids, and carbohydrates (7–11). In the high-frequency region of the ^1H spectra, resonances from the H4 and H2 protons of the imidazole ring in histidine have been reported at ~7.2 and ~8.4 ppm, respectively (11–17). Moreover, additional resonances at ~8.3–8.5 ppm have been reported (11–15, 17) and assigned to the H2 and H8 protons in ATP (12–15). However, this assignment was later questioned because of quantitative discrepancies with ATP levels determined from ^{31}P NMR spectra (17), and accordingly the

assignment of these resonances remains an unsolved matter. Likewise, a resonance at ~6.7 ppm has often been reported in ^1H NMR studies of muscle tissue (11, 13, 15, 17) and has been assigned to the protons of the amino groups in creatine (13, 15). However, because this resonance is observed only occasionally (11, 17), the origin of this resonance is not fully understood.

Magic-angle spinning (MAS), where contributions from magnetic susceptibility, dipolar coupling, and chemical shift anisotropy (CSA) are eliminated (18), leads to high-resolution ^1H NMR spectra for biological tissues (1–10). However, the high spinning rates used in conventional MAS experiments, where sample spinning rates in the kilohertz range are employed to eliminate spinning sidebands from the isotropic metabolite spectrum, cause disruptions of cell structures and severe tissue damage (2, 19, 20). Recently, the method of phase-altered spinning sidebands (PASS), originally developed for solid-state NMR (21), has been modified for studies of biological objects (22). This technique suppresses the spinning sidebands caused by magnetic susceptibility effects from the isotropic centerband spectrum and can be applied at substantially lower spinning rates, thus preventing structural damage to the sample studied.

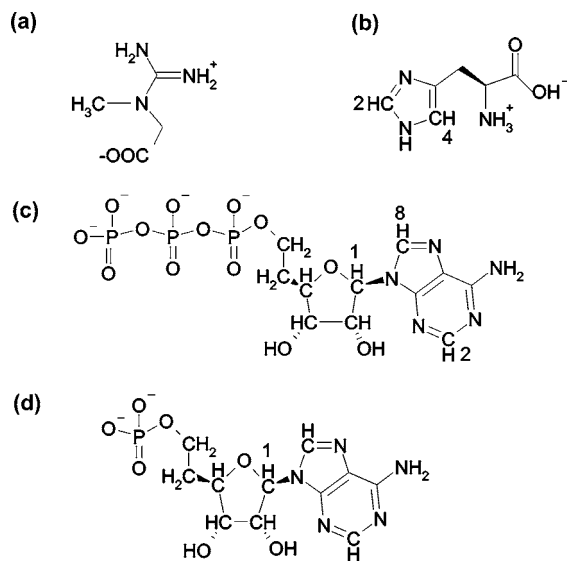
The aim of the present study is to investigate the origin of the high-frequency resonances in the ^1H MAS NMR spectra of

* Corresponding author (telephone +45 89 99 15 06; fax +45 89 99 15 64; e-mail HanneC.Bertram@agrsci.dk).

[†] Danish Institute of Agricultural Sciences.

[§] Instrument Centre for Solid-State NMR Spectroscopy, University of Aarhus.

[#] Institute of Physiology and Biophysics, University of Aarhus.

Chart 1. Chemical Structures of (a) Creatine, (b) Histidine, (c) Adenosine 5'-Triphosphate, and (d) Adenosine 5'-Monophosphate

muscle tissue employing slow-MAS PASS ^1H NMR spectroscopy to excised untreated muscle tissue, to in vitro D_2O -incubated muscle tissue, and to solutions of histidine, ATP, and creatine in $\text{H}_2\text{O}/\text{D}_2\text{O}$.

MATERIALS AND METHODS

Muscle Samples. Five-week-old Wistar rats with a live weight of ~ 125 g were sacrificed by cervical dislocation, and m. tibialis anterior muscle was immediately excised. Immediately upon excision, the intact muscle was placed in a 5 mm i.d. (7 mm o.d.) rotor used for the NMR measurements, which were started 20 min post-mortem (see below). These muscles are in the following designated untreated muscles.

To examine the effect of OH-/NH-exchangeable muscle (and H_2O) protons, muscles were preincubated in a Krebs–Ringer bicarbonate buffer (pH 7.4) based on D_2O (Cambridge Isotope Laboratories, Inc., Andover, MA) and containing 122.1 mM NaCl, 25 mM NaHCO_3 , 2.8 mM KCl, 1.2 mM KH_2PO_4 , 1.2 mM MgSO_4 , 1.3 mM CaCl_2 , and 5 mM glucose. The buffer was equilibrated with 5/95% CO_2/O_2 . The muscles were incubated at 30 °C for 2 h, and the buffer was changed each 30 min.

Individual Components. L-Histidine (0.3 M), creatine (0.4 M), and ATP/AMP (mixture, 0.04 M/0.05 M) (Sigma Chemical Co., St. Louis, MO) were dissolved separately and as mixtures in phosphate buffers based on 100% D_2O or 25/75% $\text{H}_2\text{O}/\text{D}_2\text{O}$. The pH of the phosphate buffers was adjusted to 5.5, 6.5, and 7.0, respectively. The structural formulas and numbering for the appropriate ring protons are depicted in **Chart 1**.

NMR Measurements. Slow-MAS PASS ^1H NMR experiments were performed on a Varian Unity INOVA-400 (9.4 T) spectrometer at 400 MHz. A 7 mm home-built high-speed spinning $^1\text{H}/^{19}\text{F}$ -X double-resonance probe, of similar design as recently described (23), tuned to 400 MHz, was used. In all experiments a spinning speed of 150 Hz, using a 7 mm multiple black/white marked zirconia rotor for computer rotor speed control to ± 1 Hz, was used. The two-dimensional (2D) ^1H PASS experiments were performed as described previously (22). The $\pi/2$ pulse width was 8.2 μs , and water suppression was achieved by implementing the DANTE pulse sequence prior to the start of the 2D ^1H PASS segment. The DANTE pulse sequence consisted of 4000 pulses with a flip angle of $\sim 5^\circ$ and equally spaced by 100 μs . The 2D ^1H PASS sequence with 16 evolution steps (22) was used for the measurement. For each of the 16 evolution steps a total of 16 scans was acquired with a recycle delay of 3 s, resulting in a total time of 15 min for each experiment. The 2D ^1H PASS experiments were continuously repeated 16 times to follow the post-mortem development; that is, at the end of one experiment the succeeding experiment was

Table 1. Assignment of the High-Frequency Resonances in ^1H NMR Spectra of Muscle Tissue

compound	assignment	^1H chemical shift δ (^1H) (ppm)
ATP/AMP ^a	ribose H1	6.1
creatine (phosphocreatine)	>C(NH ₂) ₂	6.7
histidine	ring H4	7.0–7.25 ^b
ATP/AMP ^a	ring H2	8.0–8.2 ^b
histidine	ring H2	8.0–8.5 ^b
ATP/AMP ^a	ring H8	8.3–8.5 ^b

^a Covers also other nucleotides and degradation products. ^b The chemical shift values are pH-dependent.

immediately started. All measurements were carried out at room temperature. The ^1H chemical shifts are relative to the internal $\text{H}_2\text{O}/\text{HOD}$ resonance being suppressed at 4.8 ppm.

Determination of pH. Using the ^1H NMR spectra, the pH of the muscle tissue was calculated from the chemical shift of the H4 proton in histidine (**Chart 1**) using eq 1 reported by Lundberg et al. (15).

$$\text{pH} = \text{p}K_a + \log \frac{\delta H - \delta}{\delta - \delta A} \quad (1)$$

Here $\text{p}K_a$ is the acid dissociation constant, δH and δA are the H4 chemical shifts of the acid and alkaline form, respectively, and δ is the actually observed chemical shift. $\text{p}K_a$ was set to 6.88, whereas δH and δA were set to 7.254 and 6.923 ppm (15), respectively. The relative increase in lactate was determined from the changes in the area of the 1.3 ppm resonance by subtraction of the first spectrum.

RESULTS

The assignments for the high-frequency resonances obtained for the muscle samples investigated in this work (vide infra) are summarized in **Table 1**.

Muscle Samples. **Figure 1** shows typical slow-MAS PASS ^1H NMR spectra obtained for an untreated and a D_2O -incubated m. tibialis anterior at 20 and 160 min post-mortem. In the region from 0 to 4 ppm several resonances are detected, the most dominating being the resonance at 1.3 ppm, which originates from methylene (CH_2) groups in lipids and the methyl (CH_3) group in lactate. During the measuring period, the intensity of the 1.3 ppm resonance increases due to formation of lactate (24). The changes in lactate content and pH determined from the chemical shift of the histidine H4 proton are displayed in **Figure 2**. For the untreated muscle (**Figure 1a,b**), resonances are observed in the high-frequency region (from 5.5 to 9 ppm) at 6.3, 6.7, 7.2, 7.5, 8.2, and 8.4–8.5 ppm. During the measuring period of 4 h, the intensity of the 6.7 ppm resonance increases markedly, and the resonances at 7.2 and 7.5 ppm move slightly toward higher chemical shift values. In contrast to these observations, for the D_2O -incubated muscle (**Figure 1c,d**), resonances are observed only at the chemical shifts of 7.2 and 8.4–8.5 ppm, respectively, which likewise move slightly toward higher chemical shift values during the measuring period. The observation of the weak resonance at 5.3 ppm in the D_2O -incubated muscle (**Figure 1c,d**) results from the improved suppression of the water resonance (4.8 ppm) following D_2O incubation.

Creatine. Panels **a–c** of **Figure 3** show slow-MAS PASS ^1H NMR spectra obtained for $\text{H}_2\text{O}/\text{D}_2\text{O}$ solutions (25/75% v/v) containing creatine and with pH adjusted to 5.5, 6.5, and 7.0, respectively. The resonances observed at 3.0 and 3.9 ppm are independent of pH and are assigned to the CH_3 and CH_2 protons in creatine, respectively (see **Chart 1**). In addition, at pH 5.5 a

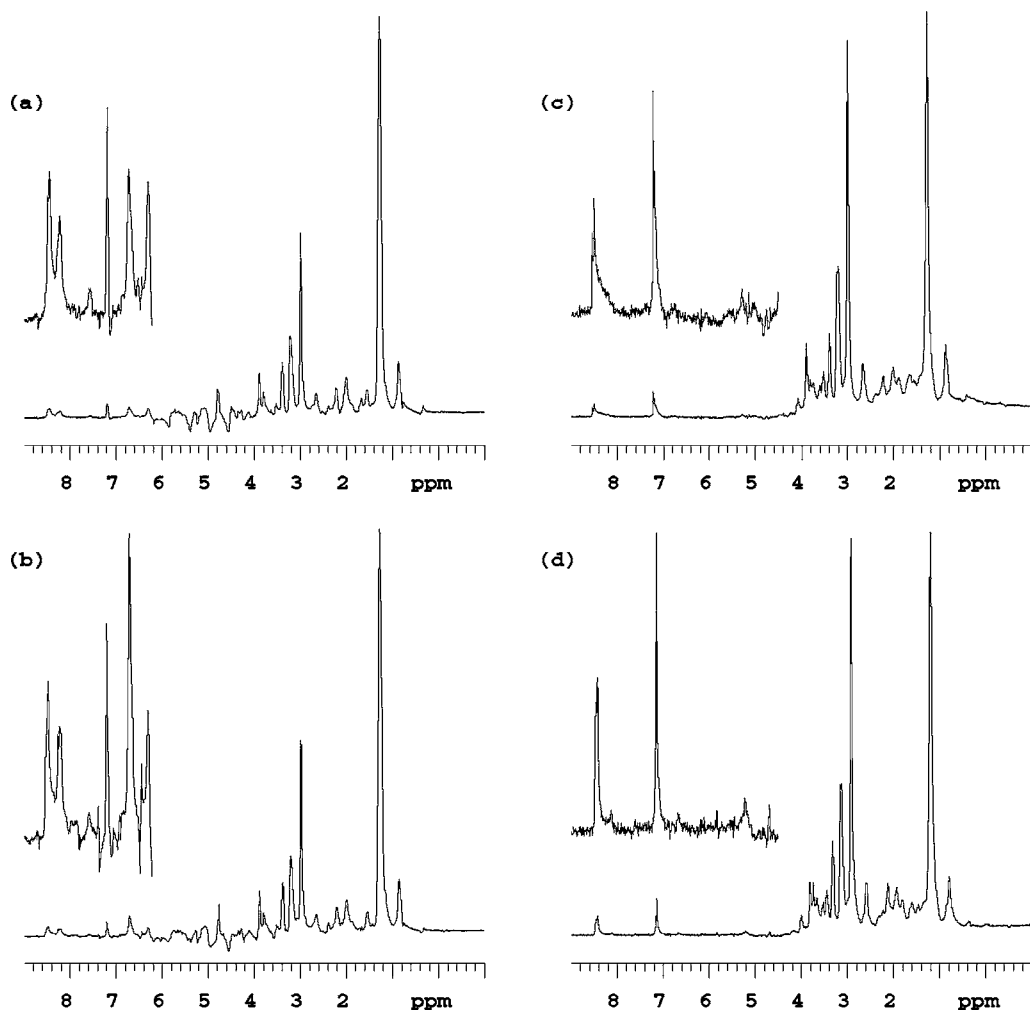


Figure 1. Slow-MAS PASS ^1H NMR spectra of rat m. tibialis anterior: (a) untreated muscle 20 min post-mortem; (b) untreated muscle 160 min post-mortem; (c) deuterium oxide-incubated muscle 20 min post-mortem; (d) deuterium oxide-incubated muscle 160 min post-mortem. Each spectrum was collected at 25 °C with a spinning frequency of 150 Hz.

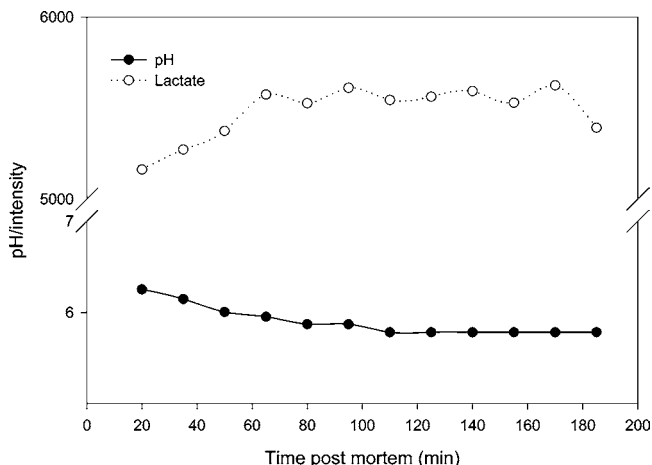


Figure 2. Development in pH and lactate content in rat m. tibialis anterior. Lactate was estimated from the increase in intensity of the 1.3 ppm resonance, and pH was calculated from the chemical shift of H4 protons in histidine.

resonance also appears at 6.7 ppm, a resonance that is absent in the spectra obtained at higher pH.

ATP and Histidine. For the pure ATP/AMP solutions (chemical structures shown in **Chart 1**) resonances are observed in the high-frequency region at 6.0 ppm (H1 in ribose), 8.0 ppm

(H2 ring), and 8.3 ppm (H8 ring) independent of pH, and, as an example, the spectrum recorded for the sample at pH 6.5 is shown in **Figure 4 a**. The splittings observed for the resonances are caused by magnetic field inhomogeneity effects attributable to vortex formation of the solution spinning at 150 Hz. This was confirmed by recording the ^1H NMR spectrum of the same solution contained in a 5 mm NMR tube on a liquid-state 200 MHz Gemini 2000 NMR spectrometer, which showed no splitting of the resonances (not shown). A PASS ^1H NMR spectrum obtained for a pure histidine solution at pH 6.5 is shown in **Figure 4b**. For the pure histidine solutions (chemical structure shown in **Chart 1**) resonances for H4 and H2 are observed at 7.1–7.2 and 8.0 ppm, respectively, in the high-frequency region, and the resonances shift toward higher chemical shift values with lower pH. **Figure 4c** displays the PASS ^1H NMR spectrum obtained for a 50:50% v/v mixture of the ATP/AMP and histidine solutions at pH 6.5. For the high-frequency region resonances are observed at 6.0, 7.1, 8.1, and 8.4 ppm.

DISCUSSION

High-resolution ^1H NMR spectroscopy has proven to be useful in studies on muscle physiology (17, 25–27), and high-resolution ^1H MAS NMR spectroscopy has also been demonstrated to be an excellent tool for the characterization of various tissues (1–10, 28–31). However, a disadvantage of MAS is

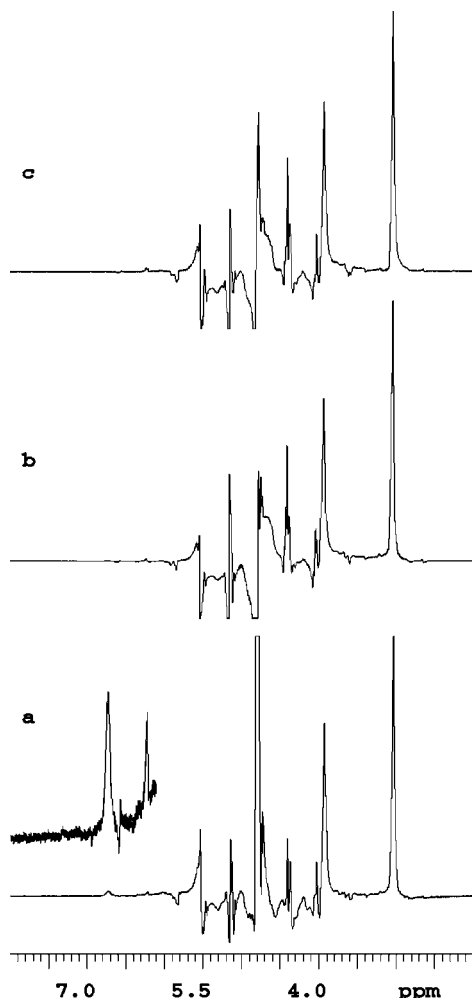


Figure 3. Slow-MAS PASS ^1H NMR spectra obtained on $\text{H}_2\text{O}/\text{D}_2\text{O}$ solutions (25/75%) containing creatine and adjusted to (a) pH 5.5, (b) pH 6.5, and (c) 7.0. Each spectrum was collected at 25 °C with a spinning frequency of 150 Hz.

the high centrifugal forces associated with the use of spinning speeds in the kilohertz range because this may cause severe damage to the samples investigated. Wind and co-workers (22) have developed a technique based on the method of phase-altered spinning sidebands, which can be employed at much lower spinning speeds, thereby preventing the damaging effect on sample integrity, and the technique has proven to be useful for studying post-mortem muscle tissue (11). In the present study we have taken advantage of this slow-MAS PASS ^1H NMR technique and have employed it to study intact, excised rat muscles. Excellent high-resolution ^1H NMR spectra (cf. **Figure 1**) have been obtained, implying that the technique is a superior tool for investigating and characterizing intact muscle tissues.

Even though ^1H NMR spectroscopy has been widely employed in studies of muscle tissues, the origin of the high-frequency resonances in the ^1H NMR spectra of such samples appears still to be a matter of dispute (17). Resonances from the H4 and H2 protons in histidine are often reported around ~ 7.0 – 7.2 and ~ 8.2 – 8.5 ppm, respectively, for muscle tissues (11–17, 27), which seem to be generally accepted. In contrast, other resonances in the high-frequency region are only observed occasionally for muscles and have been interpreted differently (11, 12, 17). The aim of the present study is to investigate the origin of these “occasional” resonances. In untreated muscle tissue, resonances are observed at 6.3, 6.7, 7.1–7.2, 7.5, 8.2,

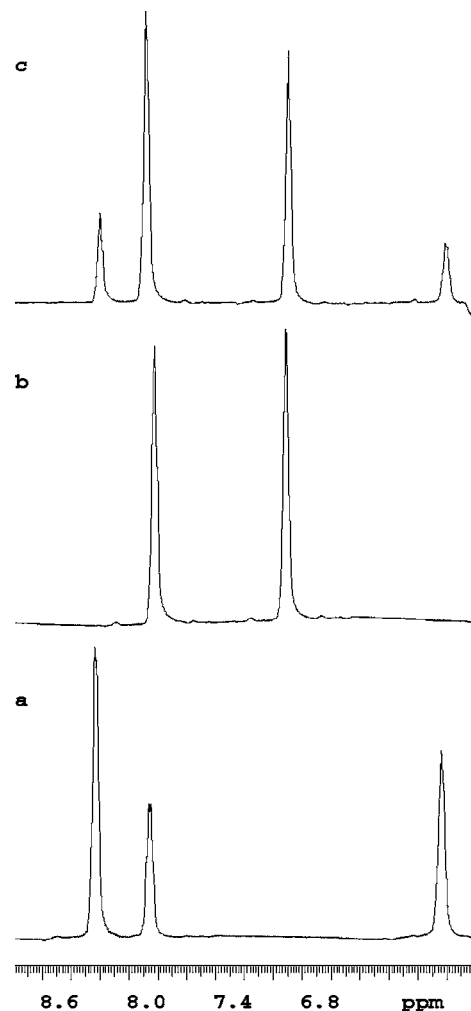


Figure 4. Slow-MAS PASS ^1H NMR spectra obtained on $\text{H}_2\text{O}/\text{D}_2\text{O}$ solutions (25/75%) at pH 6.5 containing (a) ATP/AMP (50%/50%), (b) L-histidine, and (c) a mixture of ATP/AMP (50%/50%) and L-histidine. Each spectrum was collected at 25 °C with a spinning frequency of 150 Hz.

and 8.4–8.5 ppm in the high-frequency ^1H region. The resonances at 7.1–7.2 and 8.2 ppm are confirmed to originate from the H4 and H2 protons in histidine, respectively. This is based on the facts that identical resonances are observed for the histidine solutions and that they show an expected pH dependence. The resonance around 6.7–6.8 ppm has previously been ascribed to the H4 protons in histidine located in oxidative fibers and to a pH difference between glycolytic and oxidative fibers (17). However, if for the muscle tissue both the 7.1–7.2 ppm resonance and the 6.7–6.8 ppm resonance should reflect H4 protons in histidine, this would correspond to an unrealistically high pH gradient within a muscle (see eq 1). In the present study it was observed that the 6.7–6.8 ppm resonance is absent in the muscle tissue incubated in D_2O . A difference in pH between glycolytic and oxidative fibers should not be influenced by incubation of the muscle in D_2O , and accordingly, the data obtained in the present study disagree with the suggestion (17) that the 6.7–6.8 ppm peak originates from the H4 proton in histidine residues in a less acidic environment. On the contrary, the results of the present study strongly indicate that the 6.7–6.8 ppm peak originates from amino protons, as these protons are easily exchanged by deuterium in the presence of D_2O . It is noticeable that the 6.7–6.8 ppm resonance is similar to the resonance observed in ^1H spectra of pure creatine solutions (**Figure 3**). Consequently, we propose that the 6.7–6.8 ppm

resonance originates from amino protons in creatine, which also is in accordance with previous suggestions (13, 15). Interestingly, in the spectra acquired for the untreated muscle tissues (Figure 1a,b) an increase in the intensity for the resonance at 6.7–6.8 ppm assigned to the amino protons in creatine is observed post-mortem, which most likely can be ascribed to the decrease in pH as a consequence of lactate formation and accumulation. This finding is noteworthy when the occasional appearance of the 6.7–6.8 ppm resonance is considered, as can be explained by differences in pH for the studied muscle samples. This is in accordance with the appearance of the 6.7–6.8 ppm resonance during exercise (17), where a decrease in pH is likewise taking place. A pH dependency of the intensity of the resonance from the amino protons at 6.7–6.8 ppm is also further supported by the spectra acquired for the creatine solutions (Figure 3), which show increased intensity with decreasing pH. The pH dependency of the resonance from the amino protons in creatine at 6.7–6.8 ppm should probably be ascribed to a pH-dependent exchange rate, causing a pH-dependent “NMR visibility”. Finally, it should be mentioned that the resonances ascribed to creatine may originate from both creatine and phosphocreatine in the muscles, which will have identical resonances in the ^1H NMR spectrum.

Comparison of the resonances from the H2 and H4 protons in histidine in the ^1H spectra of muscle tissue (Figure 1) implies that there is a contribution from more than the H2 protons in histidine to the resonances observed in the region 8.2–8.5 ppm. Nucleotides have resonances in this region (9, 12, 14, 15, 24), which is also demonstrated in the present study (Figure 4). As adenosine phosphates (ATP, ADP, and AMP) are known to be present in muscles, it is proposed that adenosine phosphates (H2 and H8 ring protons, Chart 1) also contribute to the resonances in the region 8.2–8.4 ppm in the ^1H NMR spectra of muscle tissue. This is supported by the ^1H spectra obtained on mixtures of ATP/AMP and histidine, which reveal that resonances from H2 in histidine and protons of ATP overlap. Table 1 summarizes the assignment for the resonances in the high-frequency region of slow-MAS PASS ^1H NMR spectra for the intact muscle tissues.

For muscles incubated in D_2O , a low-intensity resonance is observed around 5.3 ppm in the ^1H spectra because of a lower water content and thereby improved water suppression for these muscle samples (Figure 1c). This 5.3 ppm resonance is tentatively ascribed to the H1 proton in α -glucose/glycogen (7–9, 30). Detection of this resonance could be of interest in future studies, as glucose and glycogen are important metabolites in muscles through their action in glycolysis because of the great interest in understanding the properties of these metabolites in relation to exercise-induced depletion of energy stores (32–34). Lactate, formed as a consequence of anaerobic glycolysis, is another key metabolite, as it, among other factors, affects the pH of the muscles. Using the intensity of the 1.3 ppm resonance originating from methylene protons in lipids and methyl protons in lactate, the present study has demonstrated an expected increase in lactate post-mortem. Further studies are needed to confirm the use of the present methodology to study glycogen, glucose, and lactate metabolites in muscles.

In conclusion, the present study has demonstrated that excellent high-resolution ^1H NMR spectra for excised muscle tissue can be obtained by employing slow magic-angle spinning (150 Hz) PASS ^1H NMR spectroscopy. To investigate the origin of the high-frequency resonances in such high-resolution ^1H NMR spectra of muscle tissues, measurements have also been performed on muscle tissue incubated in D_2O and for $\text{H}_2\text{O}/$

D_2O solutions of histidine, ATP/AMP, and creatine. On the basis of these results it is proposed that the resonances at ~ 7.1 – 7.2 ppm originate from H4 protons in histidine and the resonances at ~ 8.2 – 8.5 ppm from H2 protons in histidine/nucleotide moieties. Finally, a resonance at 6.7–6.8 ppm exhibits pH dependence and exchanges its protons for deuterium in D_2O ; it is therefore proposed to originate from the amino protons in creatine.

ACKNOWLEDGMENT

Rigmor Sjøberg Johansen is thanked for excellent technical assistance. The use of the facilities at the Instrument Centre for Solid-State NMR Spectroscopy, University of Aarhus, sponsored by the Danish Natural Research Council, the Danish Technical Science Research Council, Teknologistyrelsen, Carlsbergfondet, and Direktør Ib Henriksens Fond, is acknowledged.

LITERATURE CITED

- (1) Cheng, L. L.; Lean, C. L.; Bogdanova, A., Jr.; Wright, S. C.; Ackerman, J. L.; Brady, T. J.; Garrido, L. Enhanced resolution of proton NMR spectra of malignant lymph nodes using magic angle spinning. *Magn. Reson. Med.* **1996**, *36*, 653–658.
- (2) Cheng, L. L.; Ma, M. J.; Becerra, L.; Hale, T.; Tracey, I.; Lackner, A.; Gonzalez, R. G. Quantitative neuropathology by high-resolution magic angle spinning proton magnetic resonance spectroscopy. *Proc. Natl. Acad. Sci. U.S.A.* **1997**, *94*, 6408–6413.
- (3) Moka, D.; Vorreuther, R.; Schicha, H.; Spraul, M.; Humpfer, E.; Lipinski, M.; Foxall, P. J. D.; Nicholson, J. K.; Lindon, J. C. Magic angle spinning proton nuclear magnetic resonance spectroscopic analysis of intact kidney tissue samples. *Anal. Commun.* **1997**, *34*, 107–109.
- (4) Moka, D.; Vorreuther, R.; Schicha, H.; Spraul, M.; Humpfer, E.; Lipinski, M.; Foxall, P. J. D.; Nicholson, J. K.; Lindon, J. C. Biochemical classification of kidney carcinoma biopsy samples using magic angle spinning ^1H nuclear magnetic resonance spectroscopy. *J. Pharm. Biomed. Anal.* **1998**, *17*, 125–132.
- (5) Humpfer, E.; Spraul, M.; Lipinski, M.; Nicholls, A. W.; Nicholson, J. K.; Lindon, J. C. Direct observation of resolved intracellular and extracellular water signals in intact human red blood cells using ^1H MAS NMR spectroscopy. *Magn. Reson. Med.* **1997**, *38*, 334–336.
- (6) Tomlins, A. M.; Foxall, P. J. D.; Lindon, J. C.; Lynch, M. L.; Spraul, M.; Everett, J. R.; Nicholson, J. K. High-resolution MAS ^1H NMR analysis of intact prostatic hyperplastic and tumor tissues. *Anal. Commun.* **1998**, *35*, 113–115.
- (7) Bollard, M. E.; Garrod, S.; Holmes, E.; Lindon, J. C.; Humpfer, E.; Spraul, M.; Nicholson, J. K. High-resolution ^1H and ^1H - ^{13}C magic angle spinning NMR spectroscopy of rat liver. *Magn. Reson. Med.* **2000**, *44*, 201–207.
- (8) Garrod, S.; Humpfer, E.; Spraul, M.; Connor, S. C.; Polley, S.; Connelly, J.; Lindon, J. C.; Nicholson, J. K.; Holmes, E. High-resolution magic angle spinning ^1H NMR spectroscopic studies on intact rat renal cortex and medulla. *Magn. Reson. Med.* **1999**, *41*, 1108–1118.
- (9) Sitter, B.; Sonnewald, U.; Spraul, M.; Fjøsne, H. E.; Gribbestad, I. S. High-resolution magic angle spinning MRS of breast cancer tissue. *NMR Biomed.* **2002**, *15*, 327–337.
- (10) Mahon, M. M.; deSouza, N. M.; Dina, R.; Soutter, W. P.; McIndoe, G. A.; Williams, A. D.; Cox, I. J. Preinvasive and invasive cervical cancer: an ex vivo proton magic angle spinning magnetic resonance spectroscopic study. *NMR Biomed.* **2004**, *17*, 144–153.
- (11) Bertram, H. C.; Hu, J. Z.; Rommereim, D. N.; Wind, R. A.; Andersen, H. J. Dynamic high-resolution ^1H and ^{31}P NMR spectroscopy and ^1H T_2 measurements in post mortem rabbit muscles using slow magic angle spinning. *J. Agric. Food Chem.* **2004**, *52*, 2681–2688.

- (12) Yoshizaki, K.; Seo, Y.; Nishikawa, H. High-resolution proton magnetic resonance spectra of muscle. *Biochim. Biophys. Acta* **1981**, *678*, 283–291.
- (13) Arús, C.; Bárány, M.; Westler, W. M.; Markley, J. L. ¹H NMR of intact muscle at 11 T. *FEBS Lett.* **1984**, *165*, 231–237.
- (14) Arús, C.; Bárány, M. Application of high-field ¹H-NMR spectroscopy for the study of perfused amphibian and excised mammalian muscles. *Biochim. Biophys. Acta* **1986**, *886*, 411–424.
- (15) Lundberg, P.; Vogel, H. J.; Ruderus, H. Carbon-13 and proton NMR studies of post-mortem metabolism in bovine muscles. *Meat Sci.* **1986**, *18*, 133–160.
- (16) Pan, J. W.; Hamm, J. R.; Rothman, D. L.; Schulman, R. G. Intracellular pH in human skeletal muscle by ¹H NMR. *Proc. Natl. Acad. Sci. U.S.A.* **1988**, *85*, 7836–7839.
- (17) Damon, B. M.; Hsu, A. C.; Stark, H. J.; Dawson, M. J. The carnosine C-2 proton's chemical shift reports intracellular pH in oxidative and glycolytic muscle fibers. *Magn. Reson. Med.* **2003**, *49*, 233–240.
- (18) Andrew, E. R.; Eades, R. G. Removal of dipolar broadening of NMR spectra of solids by specimen rotation. *Nature* **1959**, *183*, 1820.
- (19) Weybright, P.; Millis, K.; Campbell, N.; Cory, D. G.; Singer, S. High-resolution magic angle spinning ¹H nuclear magnetic resonance spectroscopy of intact cells. *Magn. Reson. Med.* **1988**, *39*, 337–344.
- (20) Griffin, J. L.; Bollard, M.; Nicholson, J.; Bhakoo, K. Spectral profiles of cultured neuronal and glial cells derived from HRMAS ¹H NMR spectroscopy. *NMR Biomed.* **2002**, *15*, 375–384.
- (21) Antzutkin, O. N.; Shekar, S. C.; Levitt, M. H. Two-dimensional sideband separation in magic-angle spinning NMR. *J. Magn. Reson.* **1995**, *A115*, 7–19.
- (22) Wind, R. A.; Hu, J. Z.; Rommereim, D. N. High-resolution ¹H NMR spectroscopy in organs and tissues using slow magic angle spinning. *Magn. Reson. Med.* **2001**, *46*, 213–218.
- (23) Jakobsen, H. J.; Daugaard, P.; Hald, E.; Rice, D.; Kupce, E.; Ellis, P. C. A 4-mm probe for ¹³C CP/MAS NMR solids at 21.15 T. *J. Magn. Reson.* **2002**, *156*, 152–154.
- (24) Bertram, H. C.; Whittaker, A. K.; Andersen, H. J.; Karlsson, A. H. The use of simultaneous ¹H and ³¹P magic angle spinning nuclear magnetic resonance measurements to characterize energy metabolism during the conversion of muscle to meat. *Int. J. Food Sci. Technol.* **2004**, *39*, 661–670.
- (25) Sharma, U.; Atri, S.; Sharma, M. C.; Sarkar, C.; Jagannathan, N. R. Skeletal muscle metabolism in Duhenne muscular dystrophy (DMD): an in-vitro proton NMR spectroscopy study. *Magn. Reson. Imaging* **2003**, *21*, 213–224.
- (26) Lebon, V.; Brillault-Salvat, C.; Bloch, G.; Leroy-Willig, A.; Carlier, P. G. Evidence of muscle BOLD effect revealed by simultaneous interleaved gradient-echo NMRI and myoglobin NMRS during leg ischemia. *Magn. Reson. Med.* **1998**, *40*, 551–558.
- (27) Bongers, H.; Schick, F.; Skalej, M.; Jung, W.-I.; Stevens, A. Localized in vivo ¹H spectroscopy of human skeletal muscle: normal and pathologic findings. *Magn. Reson. Imaging* **1997**, *10*, 957–964.
- (28) Swanson, M. G.; Vigneron, D. B.; Tabatabai, Z. L.; Males, R. G.; Schmitt, L.; Carroll, P. R.; James, J. K.; Hurd, R. E.; Kurbanewicz, J. Proton HR-MAS spectroscopy and quantitative pathologic analysis of MRI/3D-MRSI-targeted postsurgical prostate tissues. *Magn. Reson. Med.* **2003**, *50*, 944–954.
- (29) Wu, C.-L.; Taylor, J. L.; He, W.; Zepeda, A. G.; Halpern, E. F.; Bielecki, A.; Gonzalez, R. G.; Cheng, L. L. Proton high-resolution magic angle spinning NMR analysis of fresh and previously frozen tissue of human prostate. *Magn. Reson. Med.*, **2003**, *50*, 1307–1311.
- (30) Rooney, O. M.; Troke, J.; Nicholson, J. K.; Griffin, J. L. High-resolution diffusion and relaxation-edited magic angle spinning ¹H NMR spectroscopy of intact liver tissue. *Magn. Reson. Med.*, **2003**, *50*, 925–930.
- (31) Taylor, J. L.; Wu, C. L.; Cory, D.; Gonzalez, R. G.; Bielecki, A.; Cheng, L. L. High-resolution magic angle spinning proton NMR analysis of human prostate tissue with slow spinning rates. *Magn. Reson. Med.* **2003**, *50*, 627–632.
- (32) Adamo, K. B.; Graham, T. E. Comparison of traditional measurements with macroglycogen and proglycogen analysis of muscle glycogen. *J. Appl. Physiol.* **1998**, *84*, 908–913.
- (33) Asp, S.; Daugaard, J. R.; Rohde, T.; Adamo, K.; Graham, T. Muscle glycogen accumulation after a marathon: roles of fiber type and pro- and macroglycogen. *J. Appl. Physiol.* **1999**, *86*, 474–478.
- (34) Graham, T. E.; Adamo, K. B.; Shearer, J.; Marchand, I.; Saltin, B. Pro- and macroglycogenolysis: relationship with exercise intensity and duration. *J. Appl. Physiol.* **2001**, *90*, 873–879.

Received for review December 17, 2004. Revised manuscript received February 16, 2005. Accepted February 18, 2005. We are grateful to the Danish Veterinary and Agricultural Research Council (SJVF 9702805) for financial support through the project "Characterization of basic NMR properties in perimortal muscles and meat in relation to physical and metabolic changes".

JF047868J